Protective Efficacy of Gastrointestinal SARS-CoV-2 Delivery against Intranasal and Intratracheal SARS-CoV-2 Challenge in Rhesus Macaques

Jingyou Yu,[a] Natalie D. Collins,[b] Noe B. Mercado,[a] Katherine McMahan,[a] Abishek Chandrashekar,[a] Jinyan Liu,[a] Tochi Anioke,[a] Aiquan Chang,[a,c] Victoria M. Giffin,[a] David L. Hope,[a] Daniel Sellers,[a] Felix Nampanya,[a] Sarah Gardner,[a] Julia Barrett,[a] Huahua Wan,[a] Jason Velasco,[e] Elyse Teow,[e] Anthony Cook,[e] Alex Van Ry,[e] Laurent Pessaint,[e] Hanne Andersen,[e] Mark G. Lewis,[e] Christian Hofer,[g] Donald S. Burke,[f] Erica K. Barkei,[g] Hannah A. D. King,[h,i] Caroline Subra,[h,i] Diane Bolton,[h,i] Kayvon Modjarrad,[j] Nelson L. Michael,[k] Dan H. Barouch[a,c,d]

aCenter for Virology and Vaccine Research, Beth Israel Deaconess Medical Center, Harvard Medical School, Boston, Massachusetts, USA
bWalter Reed National Military Medical Center, Bethesda, Maryland, USA
cHarvard Medical School, Boston, Massachusetts, USA
dRagon Institute of MGH, MIT, and Harvard, Cambridge, Massachusetts, USA
eBioqual, Rockville, Maryland, USA
fGraduate School of Public Health, University of Pittsburgh, Pittsburgh, Pennsylvania, USA
gVeterinary Services Program, Center for Enabling Capabilities, Walter Reed Army Institute for Research, Silver Spring, Maryland, USA
hHenry Jackson Foundation, Bethesda, Maryland, USA
iMilitary HIV Research Program, Center for Infectious Disease Research, Walter Reed Army Institute for Research, Silver Spring, Maryland, USA
jEmerging Infectious Diseases Branch, Center for Infectious Disease Research, Walter Reed Army Institute for Research, Silver Spring, Maryland, USA
kCenter for Infectious Disease Research, Walter Reed Army Institute for Research, Silver Spring, Maryland, USA

Jingyou Yu and Natalie D. Collins are co-first authors. The order of the names was determined by contribution to the data generation.

ABSTRACT Live oral vaccines have been explored for their protective efficacy against respiratory viruses, particularly for adenovirus serotypes 4 and 7. The potential of a live oral vaccine against severe acute respiratory syndrome coronavirus 2 (SARS-CoV-2), however, remains unclear. In this study, we assessed the immunogenicity of live SARS-CoV-2 delivered to the gastrointestinal tract in rhesus macaques and its protective efficacy against intranasal and intratracheal SARS-CoV-2 challenge. Postpyloric administration of SARS-CoV-2 by esophagogastroduodenoscopy resulted in limited virus replication in the gastrointestinal tract and minimal to no induction of mucosal antibody titers in rectal swabs, nasal swabs, and bronchoalveolar lavage fluid. Low levels of serum neutralizing antibodies were induced and correlated with modestly diminished viral loads in nasal swabs and bronchoalveolar lavage fluid following intranasal and intratracheal SARS-CoV-2 challenge. Overall, our data show that postpyloric inoculation of live SARS-CoV-2 is weakly immunogenic and confers partial protection against respiratory SARS-CoV-2 challenge in rhesus macaques.

IMPORTANCE SARS-CoV-2 remains a global threat, despite the rapid deployment but limited coverage of multiple vaccines. Alternative vaccine strategies that have favorable manufacturing timelines, greater ease of distribution, and improved coverage may offer significant public health benefits, especially in resource-limited settings. Live oral vaccines have the potential to address some of these limitations; however, no studies have yet been conducted to assess the immunogenicity and protective efficacy of a live oral vaccine against SARS-CoV-2. Here, we report that oral administration of live SARS-CoV-2 in nonhuman primates may offer prophylactic benefits, but the formulation and route of administration will require further optimization.

Coronavirus disease 2019 (COVID-19) has claimed millions of lives since its emergence in late 2019. Rapid and broad deployment of safe, effective and affordable vaccines will be the key to end the pandemic (1, 2). Multiple severe acute respiratory syndrome coronavirus 2 (SARS-CoV-2) vaccines—including two mRNA vaccines and two adenovirus-vectored vaccines—have advanced to emergency authorization or full approval at an unprecedented pace. Yet the wide gap in global availability of vaccines and the emergence of virus variants necessitate additional vaccine approaches (1).

Live oral vaccines have long been explored for their utility to curb infectious diseases. Immunologically, the gastrointestinal (GI) tract is one of the largest lymphoid organs in the body, comprised of organized lymphoid tissue and large populations of scattered innate and adaptive effector cells, including IgA-secreting plasma cells, CD4$^+$ and CD8$^+$ T cells, regulatory T cells, and $\gamma\delta$ T cells (3, 4). Orally administered live vaccines may therefore elicit different immune responses than nonreplicating gene-based vaccines, and the GI delivery route may be a means of attenuation (5). Direct administration of antigens at mucosal surfaces is an efficient approach to inducing a potent mucosal immune response (6). Logistically, live oral vaccines allow for simplified development, rapid production and distribution, and ease of administration (7). Live virus production can be scaled up in cell culture systems without the need for complex inactivation and purification steps. Vaccination procedures are free of needles, and there is often no need for specially trained medical personnel (8). Moreover, live oral vaccines are typically cost-effective. The replicating feature of live viruses can allow for administration of a lower dose to achieve immunity. As such, oral vaccines may be preferable in resource-limited settings.

To date, several human oral vaccines have been licensed that contain live viruses. The U.S. Department of Defense (DoD) and National Institutes of Health (NIH) developed coadministered live oral vaccines against adenovirus serotypes 4 and 7 (Ad4 and Ad7) in the 1970s (9, 10) and again in 2011 when the vaccine was remanufactured (11–13). These two vaccines contain wild-type virus with an enteric coating to protect against degradation from the low pH of gastric acid as they pass through to the lower GI tract (12, 14, 15). GI administration of Ad4 and Ad7 attenuates the viruses and induces serum neutralizing antibodies (NAbs) that protect against subsequent type-specific respiratory infection (12, 14, 15). Both vaccines have been shown to be safe, do not disseminate systemically—evident by absence of vaccine virus in blood or urine—and provide more than 90% efficacy over the course of 8 to 10 weeks (11, 12, 14, 15). Recent data have revealed that the Ad4/Ad7 live oral vaccine-elicited immune responses are durable for at least 6 years (16). Oral vaccines have also been developed for GI viruses, such as rotavirus and poliovirus, which have been in use for decades in children and have consistently demonstrated high safety, immunogenicity, and efficacy profiles (17–20).

Given the success of the live oral Ad4 and Ad7 vaccines and the demonstration of the presence of the angiotensin-converting enzyme 2 (ACE2) receptor, the primary receptor for SARS-CoV-2, throughout the GI tract mucosa (21), we performed a proof-of-concept study to assess the immunogenicity and protective efficacy of GI delivery of live SARS-CoV-2 in rhesus macaques. Delivery of 1×10^6 50% tissue culture infectious doses (TCID$_{50}$) virus to the duodenum by endoscopy caused a transient infection with localized replication in the GI tract and was associated with modest immunogenicity and partial protection against intranasal (i.n.) and intratracheal (i.t.) SARS-CoV-2 challenge.

RESULTS

Limited SARS-CoV-2 replication in the gastrointestinal tract. To determine the immunogenicity and protective efficacy of the GI delivery of SARS-CoV-2, we inoculated 21 rhesus macaques with 1×10^6 50% TCID$_{50}$ SARS-CoV-2 from the WA1/2020 strain (NR-52281; BEI Resources) ($n = 9$) or phosphate-buffered saline (PBS) sham controls

(n = 12) by esophagogastroduodenoscopy (EGD). The virus inoculum was 2 mL of live virus in PBS and was delivered to the proximal duodenum on day 0.

Viral shedding was quantified on study days 1, 2, 4, 7, 14, 21 and 28 by genomic (gRNA) or envelope (E) subgenomic RNA (sgRNA) reverse transcription-PCR (RT-PCR) assays (22). Viral shedding in the stool was observed in 7 out of 9 vaccinated macaques by gRNA assays on day 1 postinoculation, but only one macaque had sustained viral shedding in stool for more than 21 days (Fig. 1A). Additionally, virus was observed by gRNA assays from rectal swabs (RS) in 4 out of 9 macaques, with detectable virus in 2 macaques at 21 days postimmunization (Fig. 1B). In contrast, virus was not detected in sham control macaques (Fig. 1A and B). Similar but limited viral shedding was observed by sgRNA assays in the vaccinated animals but not the sham controls (Fig. 1C and D). However, we did not observe virus in serum, saliva, bronchoalveolar lavage (BAL) fluid, or nasal swabs (NS) (data not shown). On day 1, vaccinated animals had a median of 3.49 $\log_{10}$ viral copies per g stool, whereas the sham animals had no detectable virus ($P < 0.00001$, two-sided Mann-Whitney tests) (Fig. 1E, left panel). In contrast, both vaccinated and sham animals had no detectable subgenomic viral RNAs in stool (Fig. 1E, right panel). These data suggest that the virus inoculum was rapidly excreted, with limited virus replication in the GI tract.

Immunogenicity of GI delivery of SARS-CoV-2 live vaccine in rhesus macaques. Four weeks after vaccination, we observed low serum pseudovirus neutralizing antibody (NAb) titers in 7 of 9 vaccinated macaques (Fig. 2), whereas the sham animals had undetectable NAb titers. Binding antibody titers determined by enzyme-linked immunosorbent assay (ELISA) and pseudovirus NAb titers in mucosal specimens, including NS, BAL fluid, RS, and stool, were below the limit of detection (data not shown). We assessed T cell responses in peripheral blood mononuclear cells (PBMCs) at week 4 postinoculation and found undetectable responses to pooled spike (S) peptides in both vaccinated and unvaccinated animals by gamma interferon (IFN-γ) enzyme-linked immunosorbent spot (ELISPOT) assays and intracellular cytokine staining (ICS) assays (data not shown). Together, these data suggest that the GI delivery of SARS-CoV-2 generated modest levels of serum neutralizing antibodies but undetectable mucosal immune responses and cellular immune responses.

Protective efficacy against SARS-CoV-2 challenge. At week 4 postinoculation, all animals were challenged with 10^5 TCID$_{50}$ SARS-CoV-2 WA1/2020, administered in a 2-mL volume by the i.n. and i.t. routes. Following challenge, we assessed viral loads in the BAL fluid and NS (22, 23). High levels of sgRNA were observed in the sham controls, with a median peak of 4.79 (range, 2.61 to 5.69) $\log_{10}$ sgRNA copies/mL in BAL fluid and a median peak of 6.21 (range, 3.30 to 6.82) $\log_{10}$ sgRNA copies/swab in NS (Fig. 3A and B). Lower viral loads were observed in the vaccinated macaques (Fig. 3A and B), with 1.61- and 1.59-$\log_{10}$ reductions of median peak sgRNA in BAL fluid and NS, respectively ($P = 0.0040$ and $P = 0.0093$, two-sided Mann-Whitney tests) (Fig. 3C). These data demonstrate that the GI-delivered SARS-CoV-2 provided partial but modest protection against respiratory SARS-CoV-2 challenge.

On day 14 following challenge, histopathology revealed minimal to mild interstitial pneumonia in all animal groups, characterized by type II pneumocyte hyperplasia, perivascular inflammation and/or vasculitis of small- to medium-sized vessels, and thickening of alveolar septa by fibrin and/or mononuclear inflammatory cells (Fig. 4). No clear difference in pulmonary pathology was noted between the vaccinated animals and sham controls.

Immune correlates of protection. Given the observed protection, we assessed immune correlates of protection. As shown in Fig. 5A, the $\log_{10}$ pseudovirus NAb titer at week 4 inversely correlated with peak $\log_{10}$ sgRNA copies/mL in both BAL fluid ($R = -0.6165$, $P = 0.0029$) and NS ($R = -0.3693$, $P = 0.0994$) (Fig. 5A). The less-robust correlation with viral loads in NS compared with viral loads in BAL fluid is consistent with prior studies (24, 25). As shown in Fig. 5B, peak viral shedding in stool did not correlate with peak $\log_{10}$ sgRNA copies/mL in BAL fluid and NS.

DISCUSSION

In this study, we demonstrate that GI delivery of 1×10^6 TCID$_{50}$ SARS-CoV-2 elicited modest immune responses and provided partial protection against intranasal and intratracheal
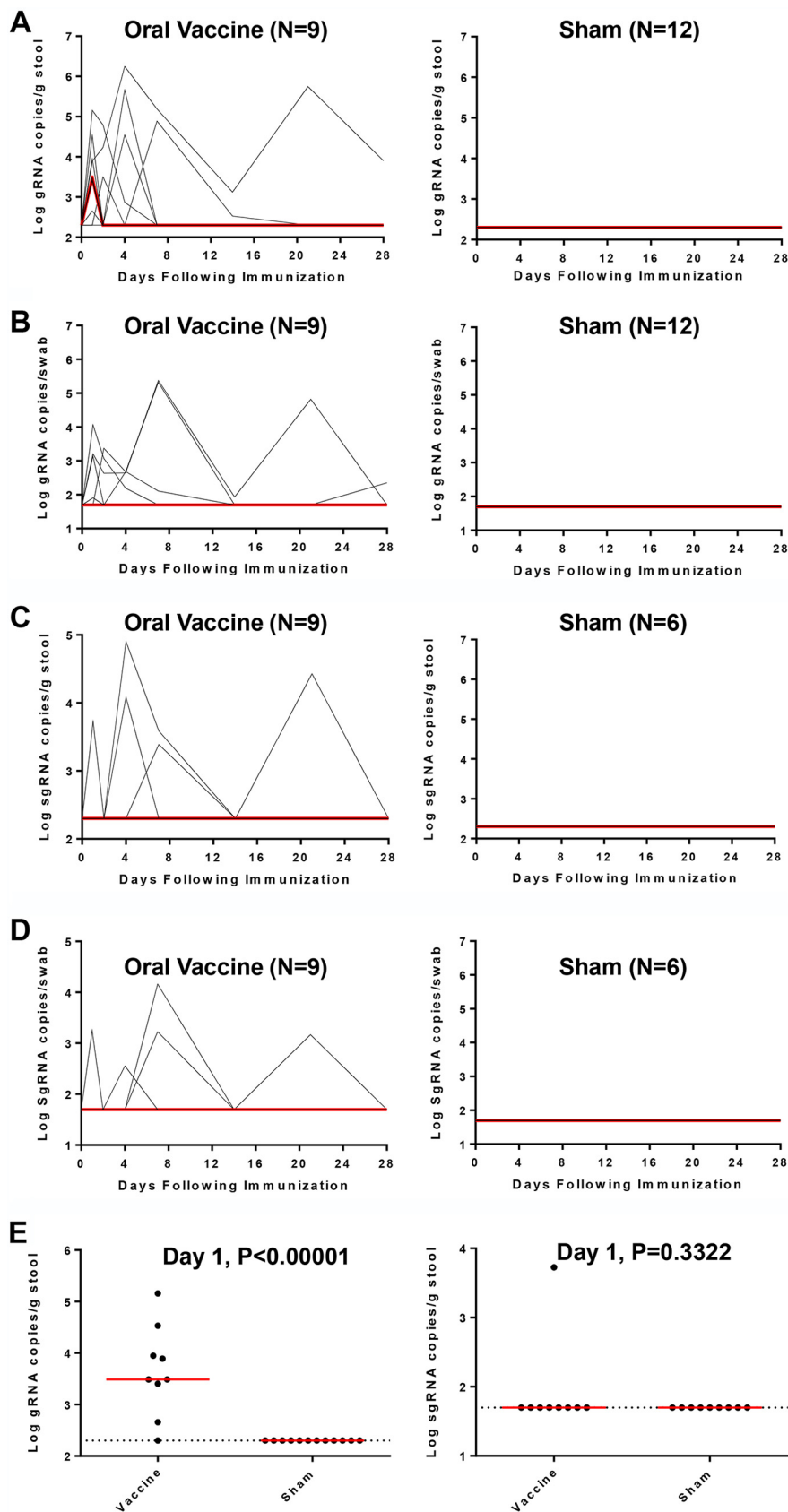
FIG 1 Viral shedding in rhesus macaques following live vaccine EGD administration. The GI of rhesus macaques was administered 10^6 TCID$_{50}$ SARS-CoV-2 via EGD. (A) Log$_{10}$ gRNA copies/g stool (limit of
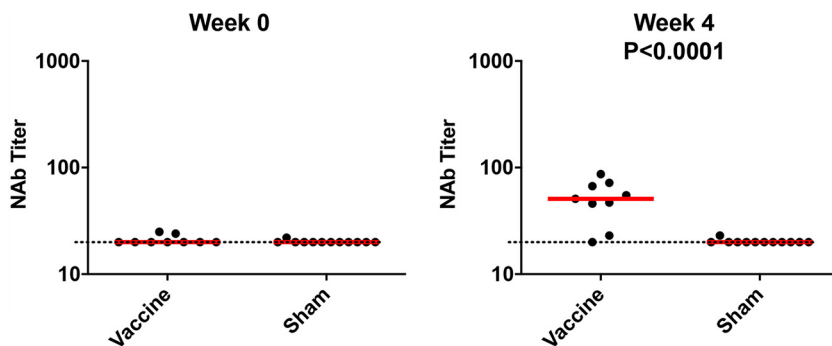
FIG 2 Humoral immune responses in vaccinated rhesus macaques. Humoral immune responses were assessed at weeks 0 and 4 by pseudovirus neutralization assays. Red bars reflect median responses. Dotted lines reflect the assay limit of detection.

challenge with SARS-CoV-2. Moreover, serum neutralizing antibody titers correlated with protective efficacy. These data provide proof of concept that an orally administered vaccine can protect against respiratory SARS-CoV-2 challenge, but the limited immunogenicity and protective efficacy observed here suggest that the oral vaccine approach will require optimization.

SARS-CoV-2 has been shown to productively infect human and macaque GI tract (26–28), specifically enterocytes (29–31), and infection is frequently associated with clinical symptoms in humans (32). We thus hypothesized that the replication of the live viral vaccine in the gut may lead to induction of systemic and mucosal immunity. We observed rapid excretion of the virus with minimal replication in the GI tract, which may explain the poor immunogenicity and limited protection. In contrast, Jiao et al. recently reported that intragastric inoculation of 1×10^7 PFU SARS-CoV-2 in rhesus macaques resulted in a productive and sustained viral infection in GI tract (28). This could reflect different inoculum doses, administration techniques, or animal cohorts.

Data on expression of ACE2 receptor in the stomach and GI tract are limited. Available data suggest abundant expression in the small intestines (21). Taken together with minimal replication of SARS-CoV2 in the GI tract, but clear correlation of serum NAb with protection in the BAL fluid and NS, it is likely that the limited immune responses were due to an inadequate antigenic load in the GI tract. Enveloped viruses such as SARS-CoV-2 would be readily destroyed by the bile secreted into the second part of duodenum, unlike nonenveloped poliovirus, adenovirus, or rotavirus vaccines. Therefore, optimization of the oral vaccine formulation, including the use of encapsulation and buffers for improved controlled delivery of SARS-CoV-2 to the GI tract, with adequate time for viral replication in a hospitable microenvironment, may allow more effective delivery of an oral vaccine. Higher doses or repetitive doses may also prove useful. In addition, nonhuman primates generally present with mild disease for SARS-CoV-2 infection, while severe disease models such as hamsters have been documented to have subclinical respiratory infection with virus shedding after oral inoculation (33). Therefore, it would be interesting to interrogate the vaccine effectiveness in different animal models.

In summary, our data show that a single postpyloric administration of live SARS-CoV-2 by EGD elicited detectable serum NAb titers and partially protected against respiratory SARS-CoV-2 challenge in rhesus macaques. Optimization of the current strategy, with encapsulation and extended delivery systems, as well as improvements in dosage and schedule, will be required for a live, oral, SARS-CoV-2 vaccine.

FIG 1 Legend (Continued)
200 copies/mL) or (C) Log_{10} sgRNA copies/g stool were assessed in stools in sham controls and in vaccinated animals following challenge. (B) Log_{10} gRNA copies/swab or (D) Log_{10} sgRNA copies/swab (limit of 50 copies/swab) were assessed in rectal swabs (RS) in sham controls and in vaccinated animals following challenge. Red lines reflect median values. (E) Peak viral loads in stool on day 1 following vaccination. Red lines reflect median viral loads. *P* values indicate two-sided Mann-Whitney tests.
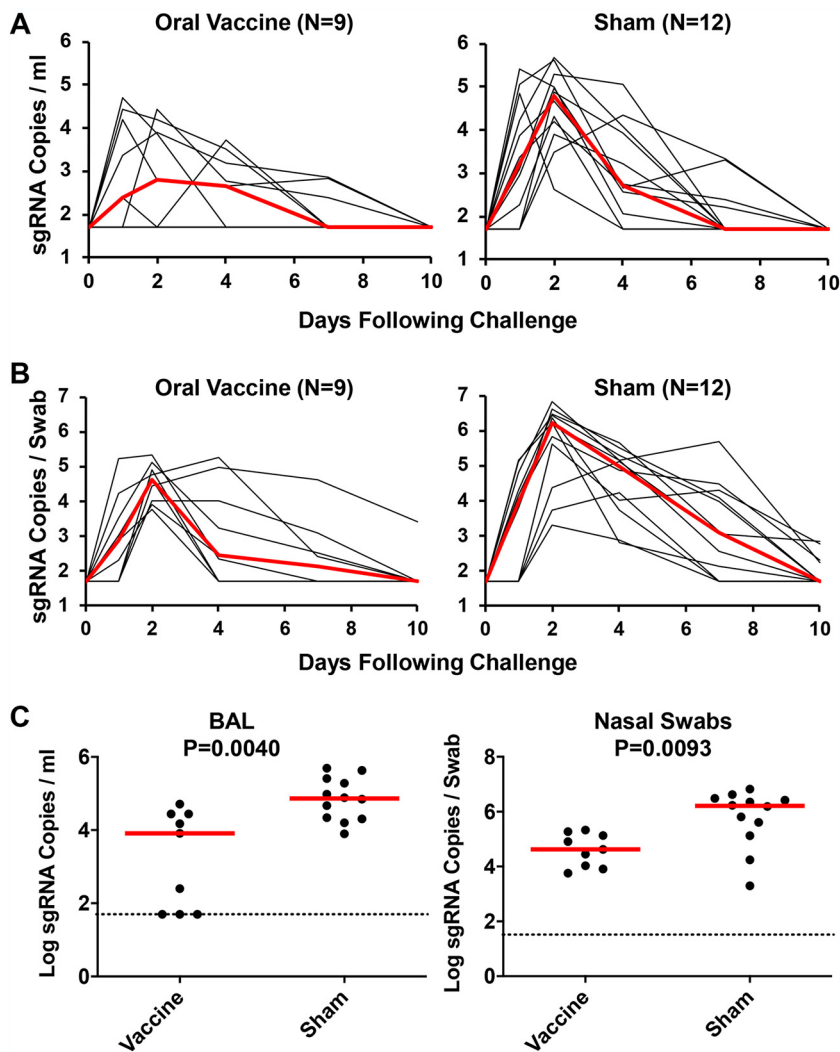
FIG 3 Viral loads in rhesus macaques following SARS-CoV-2 challenge. Rhesus macaques were challenged by the intranasal and intratracheal routes with 10^5 $TCID_{50}$ SARS-CoV-2. (A) Log_{10} sgRNA copies/mL (limit of 50 copies/mL) were assessed in bronchoalveolar lavage (BAL) fluid in sham controls and in vaccinated animals following challenge. (B) Log_{10} sgRNA copies/swab (limit of 50 copies/swab) were assessed in nasal swabs (NS) in sham controls and in vaccinated animals following challenge. Red lines reflect median values. (C) Peak viral loads in BAL fluid and NS following challenge. Peak viral loads occurred on day 2 following challenge. Red lines reflect median viral loads. *P* values indicate two-sided Mann-Whitney tests.

MATERIALS AND METHODS

Animals, virus stocks, and study design. Twenty-one outbred Indian-origin adult male and female rhesus macaques (*Macaca mulatta*) ages 6 to 14 years old were randomly allocated to groups. All animals were housed at Bioqual, Inc. (Rockville, MD). Animals were EGD administered 1×10^6 $TCID_{50}$ SARS-CoV-2 into the duodenum and then challenged with 10^5 $TCID_{50}$ of WA1/2020 on day 28. The WA1/2020 challenge stock (USA-WA1/2020; BEI Resources; NR-5228) was grown in VeroE6 cells and deep sequenced as described previously (34). Deep sequencing of these stocks revealed no mutations in the spike protein greater than >2.5% frequency. At the time of challenge, virus was administered as 1 mL by the i.n. route (0.5 mL in each nare) and 1 mL by the i.t. route. All immunologic and virologic studies were performed blind. Animal studies were conducted in compliance with all relevant local, state, and federal regulations and were approved by the Bioqual Institutional Animal Care and Use Committee (IACUC).

EGD administration. The scope was slowly and trans-orally inserted, under direct vision. Once the endoscope was in the stomach, insufflation, aspiration, and suctioning were used to aid in finding the specified gastrointestinal region (pyloric region, the duodenum, or the jejunum). Once the duodenum was identified, the inoculum was administered through the instrument channel inlet. The channel was then flushed with 1 to 2 mL of sterile water. The endoscope was removed and cleaned with appropriate disinfectant in between animals. A new endoscope was used on another animal while the previous endoscope was disinfected.
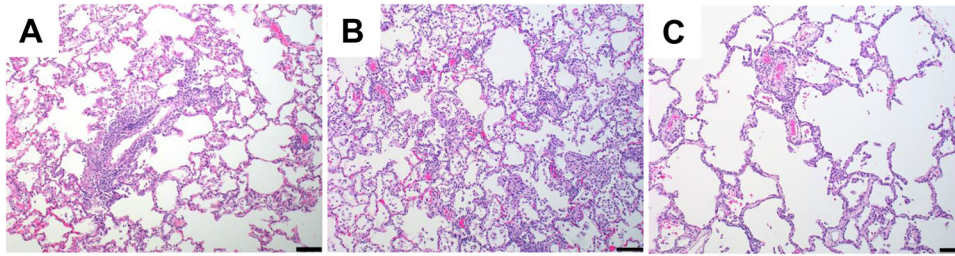
FIG 4 Histopathologic examination following SARS-CoV-2 challenge. Lung tissues were collected at necropsy on day 14 postchallenge, fixed with neutral buffered formalin, and stained with hematoxylin and eosin (H&E) for standard microscopic examination. Shown are representative lung tissue sections from the PBS control (A), high-dose (10^6 TCID$_{50}$)-vaccinated (B), and low-dose (10^4 TCID$_{50}$)-vaccinated (C) SARS-CoV-2-challenged rhesus macaques. Minimal to mild interstitial pneumonia is characterized by inflammatory cellular infiltrates and type II pneumocyte hyperplasia. Scale bars, 100 μm.

Pseudovirus-based virus neutralization assay. The SARS-CoV-2 pseudoviruses expressing a luciferase reporter gene were generated essentially as described previously (24, 25, 34, 35). Briefly, the packaging plasmid psPAX2 (AIDS Resource and Reagent Program), luciferase reporter plasmid pLenti-CMV Puro-Luc (Addgene), and spike protein expressing pcDNA3.1-SARS CoV-2 SΔCT of variants were cotransfected into HEK293T cells by Lipofectamine 2000 (Thermo Fisher). Pseudoviruses of SARS-CoV-2 variants were generated by using the Wuhan/WIV04/2019 strain (GISAID accession ID EPI_ISL_402124). The supernatants containing the pseudotype viruses were collected 48 h posttransfection, which were purified by centrifugation and filtration with 0.45-μm-pore filter. To determine the neutralization activity of the plasma or serum samples from participants, HEK293T-hACE2 cells were seeded in 96-well tissue culture plates at a density of 1.75×10^4 cells/well overnight. Three-fold serial dilutions of heat-inactivated serum or nasal swab, BAL fluid, rectal swab, or stools were prepared and mixed with 50 μL of pseudovirus. The mixture was incubated at 37°C for 1 h before being added to HEK293T-hACE2 cells. Forty-eight hours after infection, cells were lysed in Steady-Glo luciferase assay mixture (Promega) according to the manufacturer's instructions. SARS-CoV-2 neutralization titers were defined as the sample dilution at which a 50% reduction in relative light units (RLU) was observed relative to the average of the virus control wells.

ELISA. WA1/2020 RBD-specific binding antibodies were assessed by ELISA essentially as described previously (24, 25, 34). Briefly, 96-well plates were coated with 1 μg/mL RBD protein (source, Aaron Schmidt) in 1$\times$ Dulbecco's phosphate-buffered saline (DPBS) and incubated at 4°C overnight. After incubation, plates were washed once with wash buffer (0.05% Tween 20 in 1$\times$ DPBS) and blocked with 350 μL casein block/well for 2 to 3 h at room temperature. After incubation, block solution was discarded, and plates were blotted dry. Serial dilutions of heat-inactivated serum diluted in casein block were added to wells, and plates were incubated for 1 h at room temperature, prior to three further washes and 1 h of incubation with a 1-μg/mL dilution of anti-macaque IgG conjugated with horseradish peroxidase (HRP) (Nonhuman Primate Reagent Resource) or a 1:1,000 dilution of anti-monkey IgA-HRP (Novus) at room temperature in the dark. Plates were then washed three times, and 100 μL of SeraCare KPL tetramethylbenzidine (TMB) SureBlue start solution was added to each well; plate development was halted by the addition of 100 μL SeraCare KPL TMB stop solution per well. The absorbance at 450 nm was recorded using a VersaMax microplate reader. For each sample, the ELISA endpoint titer was calculated in GraphPad Prism software, using a four-parameter logistic curve fit to calculate the reciprocal serum dilution that yields an absorbance value of 0.2 at 450 nm. Log$_{10}$ endpoint titers are reported.

IFN-γ ELISPOT assay. ELISPOT assays were performed essentially as described previously (24, 25, 34). ELISPOT plates were coated with mouse anti-human IFN-γ monoclonal antibody from BD Biosciences Pharmingen at 5 μg/well and incubated overnight at 4°C. Plates were washed with DPBS wash buffer (DPBS with 0.25% Tween 20) and blocked with R10 medium (RPMI with 10% heat-inactivated fetal bovine serum [FBS] with 1% 100$\times$ penicillin-streptomycin) for 1 to 4 h at 37°C. SARS-CoV-2 peptides pools from JPT were prepared and plated at a concentration of 1 μg/well, and 200,000 cells/well were added to the plate. The peptides and cells were incubated for 18 to 24 h at 37°C. All steps following this incubation were performed at room temperature. The plates were washed with ELISPOT wash buffer (11% 10$\times$ DPBS and 0.3% Tween 20 in 1 L Milli-Q water) and incubated for 2 h with rabbit polyclonal anti-human IFN-γ conjugated with biotin from U-Cytech (1 μg/mL). The plates were washed a second time and incubated for 2 h with streptavidin-alkaline phosphatase from Southern Biotech (2 μg/mL). The final wash was followed by the addition of nitroblue tetrazolium chloride–5-bromo-4-chloro-3-indolylphosphate p-toludine salt (NBT/BCIP chromogen) substrate solution for 7 min. The chromogen was discarded, and the plates were washed with water and dried in a dark place for 24 h. Plates were scanned and counted on a Cellular Technologies Limited immunospot analyzer.

ICS assay. Multiparameter ICS assays were performed utilizing modification of described previously protocols (24, 25, 34).

gRNA and sgRNA assay. SARS-CoV-2 E gene RNA sgRNA and N gene RNA gRNA were assessed by RT-PCR using primers and probes as previously described (22, 23). A standard was generated by first synthesizing a gene fragment of the subgenomic E gene (23). The gene fragment was subsequently cloned into a pcDNA3.1+ expression plasmid using restriction site cloning (Integrated DNA Technologies). The insert
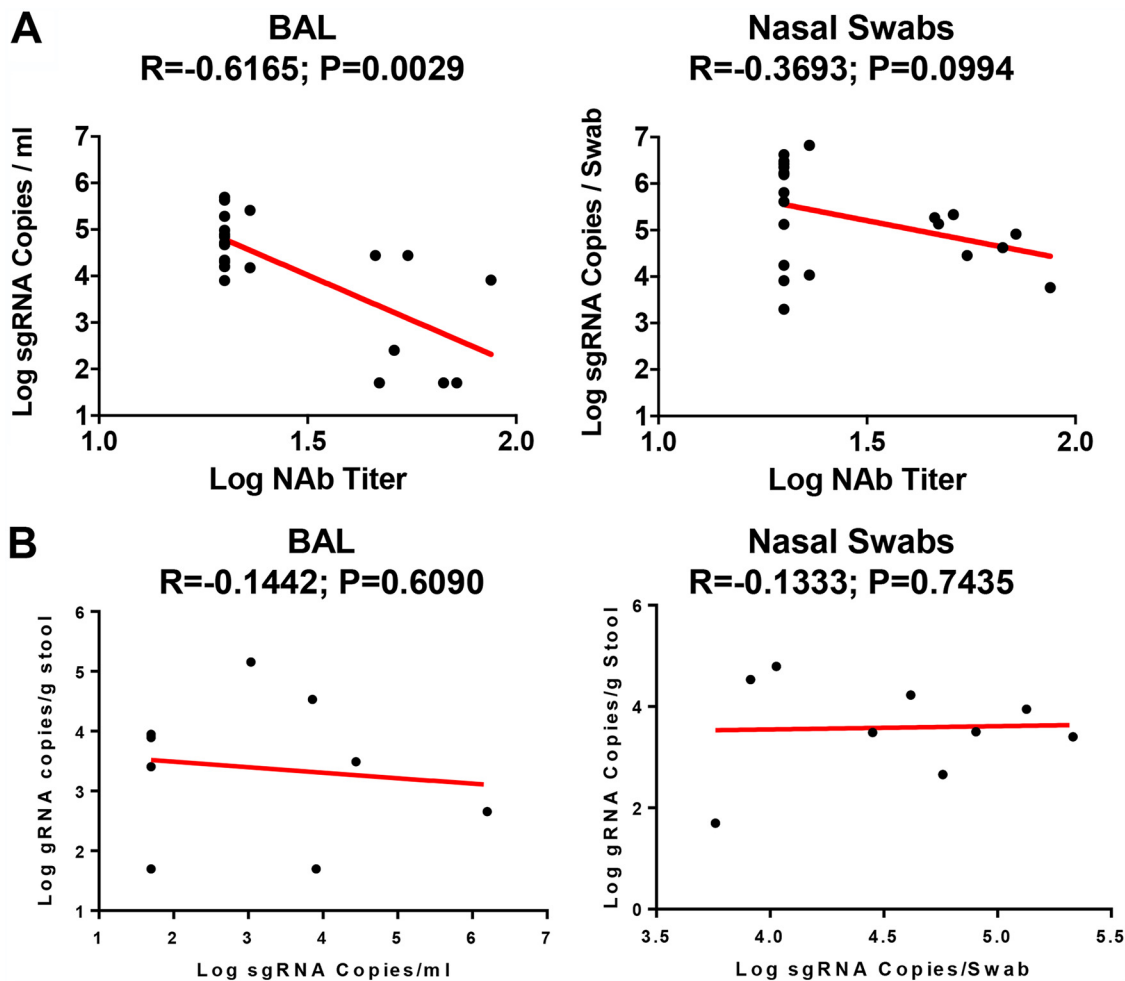
FIG 5 Immune correlates of protection. (A) Correlations of pseudovirus NAb titers at week 4 with log peak sgRNA copies/mL in BAL fluid and NS following challenge. (B) Correlations of log peak sgRNA copies/mL in BAL fluid and NS with log peak gRNA copies/g stool. Red lines reflect the best-fit relationship between these variables. *P* and *R* values reflect two-sided Spearman rank-correlation tests.

was *in vitro* transcribed to RNA using the AmpliCap-Max T7 High Yield Message Maker kit (CellScript). Log dilutions of the standard were prepared for RT-PCR assays ranging from 1×10^{10} copies to 1×10^{-1} copies. Viral loads were quantified from BAL fluid, NS, RS, and stool. RNA extraction was performed on a QIAcube HT using the IndiSpin QIAcube HT pathogen kit according to manufacturer's specifications (Qiagen). The standard dilutions and extracted RNA samples were reverse transcribed using SuperScript VILO master mix (Invitrogen) following the cycling conditions described by the manufacturer: 25°C for 10 min, 42°C for 1 h, and then 85°C for 5 min. A TaqMan custom gene expression assay (Thermo Fisher Scientific) was designed using the sequences targeting the E gene sgRNA (23). The sequences for the custom assay were as follows: sgLeadCoV2.Fwd, CGATCTCTTGTAGATCTGTTCTC; E_Sarbeco_R, ATATTGCA GCAGTACGCACACA; and E_Sarbeco_P1 (probe), VIC-ACACTAGCCATCCTTACTGCGCTTCG-MGBNFQ. SARS-CoV-2 genomic RNA (gRNA) was targeted using N gene primers and probe: 2019-nCoV_N1-F, GACCCC AAAATCAGCGAAAT; 2019-nCoV_N1-R, TCTGGTTACTGCCAGTTGAATCTG; and 2019-nCoV_N1-P, FAM (6-carboxyfluorescein)-ACCCCGCATTACGTTTGGTGGACC-BHQ1 (black hole quencher 1). Reactions were carried out in duplicate for samples and standards on the QuantStudio 6 and 7 Flex real-time PCR systems (Applied Biosystems) with the thermal cycling conditions of initial denaturation at 95°C for 20 s and then 45 cycles of 95°C for 1 s and 60°C for 20 s. Standard curves were used to calculate genomic and subgenomic RNA copies per mL or per swab; the quantitative assay sensitivity was 50 copies per mL or per swab for both genomic and subgenomic assays. Sensitivity of the stool analysis was determined as 200 copies/g of stool.

Histopathology. Necropsies were performed according to institutional animal care and use committee-approved protocols at 14 days postinfection. Lungs were perfused with 10% neutral-buffered formalin. Three tissue sections each from the right and left lung lobes were used to evaluate the lung pathology. Sections were processed routinely into paraffin wax and then sectioned at 5 μm, and the resulting slides were stained with hematoxylin and eosin. All tissue slides were evaluated by a board-certified veterinary anatomic pathologist blind to study group allocations.

Statistical analyses. Comparisons of virologic and immunologic data were performed using GraphPad Prism 8.4.2 (GraphPad Software). Comparison of data between groups was performed using two-sided Wilcoxon rank-sum tests. Correlation analyses were performed either using two-sided Spearman rank correlation tests or linear regression. *P* values of less than 0.05 were considered significant.

Animal care and use. This research was conducted under an approved animal use protocol in an AAALAC-accredited facility in compliance with the Animal Welfare Act and all other federal statutes and regulations relating to animals and experiments involving animals and adheres to principles stated in the *Guide for the Care and Use of Laboratory Animals* (36).

ACKNOWLEDGMENTS

Material has been reviewed by the Walter Reed Army Institute of Research. There is no objection to its presentation and/or publication. The opinions or assertions contained herein are the private views of the author, and are not to be construed as official, or as reflecting true views of either the Department of the Army or the Department of Defense.

REFERENCES

1. Corey L, Mascola JR, Fauci AS, Collins FS. 2020. A strategic approach to COVID-19 vaccine R&D. Science 368:948–950. https://doi.org/10.1126/science.abc5312.

2. Dagotto G, Yu J, Barouch DH. 2020. Approaches and challenges in SARS-CoV-2 vaccine development. Cell Host Microbe 28:364–370. https://doi.org/10.1016/j.chom.2020.08.002.

3. Mowat AM, Agace WW. 2014. Regional specialization within the intestinal immune system. Nat Rev Immunol 14:667–685. https://doi.org/10.1038/nri3738.

4. Holmgren J, Czerkinsky C. 2005. Mucosal immunity and vaccines. Nat Med 11:S45–S53. https://doi.org/10.1038/nm1213.

5. Robert-Guroff M. 2007. Replicating and non-replicating viral vectors for vaccine development. Curr Opin Biotechnol 18:546–556. https://doi.org/10.1016/j.copbio.2007.10.010.

6. Neutra MR, Kozlowski PA. 2006. Mucosal vaccines: the promise and the challenge. Nat Rev Immunol 6:148–158. https://doi.org/10.1038/nri1777.

7. Vela Ramirez JE, Sharpe LA, Peppas NA. 2017. Current state and challenges in developing oral vaccines. Adv Drug Deliv Rev 114:116–131. https://doi.org/10.1016/j.addr.2017.04.008.

8. Deal C, Pekosz A, Ketner G. 2013. Prospects for oral replicating adenovirus-vectored vaccines. Vaccine 31:3236–3243. https://doi.org/10.1016/j.vaccine.2013.05.016.

9. Top FH, Jr, Grossman RA, Bartelloni PJ, Segal HE, Dudding BA, Russell PK, Buescher EL. 1971. Immunization with live types 7 and 4 adenovirus vaccines. I. Safety, infectivity, antigenicity, and potency of adenovirus type 7 vaccine in humans. J Infect Dis 124:148–154. https://doi.org/10.1093/infdis/124.2.148.

10. Top FH, Jr, Dudding BA, Russell PK, Buescher EL. 1971. Control of respiratory disease in recruits with types 4 and 7 adenovirus vaccines. Am J Epidemiol 94:142–146. https://doi.org/10.1093/oxfordjournals.aje.a121306.

11. Kuschner RA, Russell KL, Abuja M, Bauer KM, Faix DJ, Hait H, Henrick J, Jacobs M, Liss A, Lynch JA, Liu Q, Lyons AG, Malik M, Moon JE, Stubbs J, Sun W, Tang D, Towle AC, Walsh DS, Wilkerson J. 2013. A phase 3, randomized, double-blind, placebo-controlled study of the safety and efficacy of the live, oral adenovirus type 4 and type 7 vaccine, in U.S. military recruits. Vaccine 31:2963–2971. https://doi.org/10.1016/j.vaccine.2013.04.035.

12. Lyons A, Longfield J, Kuschner R, Straight T, Binn L, Seriwatana J, Reitstetter R, Froh IB, Craft D, McNabb K, Russell K, Metzgar D, Liss A, Sun X, Towle A, Sun W. 2008. A double-blind, placebo-controlled study of the safety and immunogenicity of live, oral type 4 and type 7 adenovirus vaccines in adults. Vaccine 26:2890–2898. https://doi.org/10.1016/j.vaccine.2008.03.037.

13. Choudhry A, Mathena J, Albano JD, Yacovone M, Collins L. 2016. Safety evaluation of adenovirus type 4 and type 7 vaccine live, oral in military recruits. Vaccine 34:4558–4564. https://doi.org/10.1016/j.vaccine.2016.07.033.

14. Gaydos CA, Gaydos JC. 1995. Adenovirus vaccines in the U.S. military. Mil Med 160:300–304. https://doi.org/10.1093/milmed/160.6.300.

15. Hilleman MR, Stallones RA, Gauld RL, Warfield MS, Anderson SA. 1957. Vaccination against acute respiratory illness of adenovirus (RI-APC-ARD) etiology. Am J Public Health Nations Health 47:841–847. https://doi.org/10.2105/ajph.47.7.841.

16. Collins ND, Adhikari A, Yang Y, Kuschner RA, Karasavvas N, Binn LN, Walls SD, Graf PCF, Myers CA, Jarman RG, Hang J. 2020. Live oral adenovirus type 4 and type 7 vaccine induces durable antibody response. Vaccines 8:411. https://doi.org/10.3390/vaccines8030411.

17. Bandyopadhyay AS, Garon J, Seib K, Orenstein WA. 2015. Polio vaccination: past, present and future. Future Microbiol 10:791–808. https://doi.org/10.2217/fmb.15.19.

18. Jain S, Basavaraj P, Singh S, Singla A, Kundu H, Singh K. 2014. Polio eradication—lessons from the past and future perspective. J Clin Diagn Res 8:ZC56–60. https://doi.org/10.7860/JCDR/2014/8383.4621.

19. Kirkwood CD, Ma LF, Carey ME, Steele AD. 2019. The rotavirus vaccine development pipeline. Vaccine 37:7328–7335. https://doi.org/10.1016/j.vaccine.2017.03.076.

20. Glass RI, Parashar UD, Bresee JS, Turcios R, Fischer TK, Widdowson MA, Jiang B, Gentsch JR. 2006. Rotavirus vaccines: current prospects and future challenges. Lancet 368:323–332. https://doi.org/10.1016/S0140-6736(06)68815-6.

21. Hamming I, Timens W, Bulthuis MLC, Lely AT, Navis GJ, van Goor H. 2004. Tissue distribution of ACE2 protein, the functional receptor for SARS coronavirus. A first step in understanding SARS pathogenesis. J Pathol 203:631–637. https://doi.org/10.1002/path.1570.

22. Dagotto G, Mercado NB, Martinez DR, Hou YJ, Nkolola JP, Carnahan RH, Crowe JE, Baric RS, Barouch DH. 2021. Comparison of subgenomic and total RNA in SARS-CoV-2-challenged rhesus macaques. J Virol 95:e02370-20. https://doi.org/10.1128/JVI.02370-20.

23. Wolfel R, Corman VM, Guggemos W, Seilmaier M, Zange S, Muller MA, Niemeyer D, Jones TC, Vollmar P, Rothe C, Hoelscher M, Bleicker T, Brunink S, Schneider J, Ehmann R, Zwirglmaier K, Drosten C, Wendtner C. 2020. Virological assessment of hospitalized patients with COVID-2019. Nature 581:465–469. https://doi.org/10.1038/s41586-020-2196-x.

24. Yu J, Tostanoski LH, Peter L, Mercado NB, McMahan K, Mahrokhian SH, Nkolola JP, Liu J, Li Z, Chandrashekar A, Martinez DR, Loos C, Atyeo C, Fischinger S, Burke JS, Slein MD, Chen Y, Zuiani A, Lelis FJN, Travers M,

Habibi S, Pessaint L, Van Ry A, Blade K, Brown R, Cook A, Finneyfrock B, Dodson A, Teow E, Velasco J, Zahn R, Wegmann F, Bondzie EA, Dagotto G, Gebre MS, He X, Jacob-Dolan C, Kirilova M, Kordana N, Lin Z, Maxfield LF, Nampanya F, Nityanandam R, Ventura JD, Wan H, Cai Y, Chen B, Schmidt AG, Wesemann DR, Baric RS, et al. 2020. DNA vaccine protection against SARS-CoV-2 in rhesus macaques. Science 369:806–811. https://doi.org/10.1126/science.abc6284.

25. Mercado NB, Zahn R, Wegmann F, Loos C, Chandrashekar A, Yu J, Liu J, Peter L, McMahan K, Tostanoski LH, He X, Martinez DR, Rutten L, Bos R, van Manen D, Vellinga J, Custers J, Langedijk JP, Kwaks T, Bakkers MJG, Zuijdgeest D, Rosendahl Huber SK, Atyeo C, Fischinger S, Burke JS, Feldman J, Hauser BM, Caradonna TM, Bondzie EA, Dagotto G, Gebre MS, Hoffman E, Jacob-Dolan C, Kirilova M, Li Z, Lin Z, Mahrokhian SH, Maxfield LF, Nampanya F, Nityanandam R, Nkolola JP, Patel S, Ventura JD, Verrington K, Wan H, Pessaint L, Van Ry A, Blade K, Strasbaugh A, Cabus M, et al. 2020. Single-shot Ad26 vaccine protects against SARS-CoV-2 in rhesus macaques. Nature 586:583–588. https://doi.org/10.1038/s41586-020-2607-z.

26. Guo M, Tao W, Flavell RA, Zhu S. 2021. Potential intestinal infection and faecal-oral transmission of SARS-CoV-2. Nat Rev Gastroenterol Hepatol 18:269–283. https://doi.org/10.1038/s41575-021-00416-6.

27. Xiao F, Tang M, Zheng X, Liu Y, Li X, Shan H. 2020. Evidence for gastrointestinal infection of SARS-CoV-2. Gastroenterology 158:1831–1833.e3. https://doi.org/10.1053/j.gastro.2020.02.055.

28. Jiao L, Li H, Xu J, Yang M, Ma C, Li J, Zhao S, Wang H, Yang Y, Yu W, Wang J, Yang J, Long H, Gao J, Ding K, Wu D, Kuang D, Zhao Y, Liu J, Lu S, Liu H, Peng X. 2021. The gastrointestinal tract is an alternative route for SARS-CoV-2 infection in a nonhuman primate model. Gastroenterology 160:1647–1661. https://doi.org/10.1053/j.gastro.2020.12.001.

29. Lamers MM, Beumer J, van der Vaart J, Knoops K, Puschhof J, Breugem TI, Ravelli RBG, Paul van Schayck J, Mykytyn AZ, Duimel HQ, van Donselaar E, Riesebosch S, Kuijpers HJH, Schipper D, van de Wetering WJ, de Graaf M, Koopmans M, Cuppen E, Peters PJ, Haagmans BL, Clevers H. 2020. SARS-CoV-2 productively infects human gut enterocytes. Science 369:50–54. https://doi.org/10.1126/science.abc1669.

30. Zang R, Castro MFG, McCune BT, Zeng Q, Rothlauf PW, Sonnek NM, Liu Z, Brulois KF, Wang X, Greenberg HB, Diamond MS, Ciorba MA, Whelan SPJ, Ding S. 2020. TMPRSS2 and TMPRSS4 promote SARS-CoV-2 infection of human small intestinal enterocytes. Sci Immunol 5:eabc3582. https://doi.org/10.1126/sciimmunol.abc3582.

31. Hoffmann M, Kleine-Weber H, Schroeder S, Krüger N, Herrler T, Erichsen S, Schiergens TS, Herrler G, Wu N-H, Nitsche A, Müller MA, Drosten C, Pöhlmann S. 2020. SARS-CoV-2 cell entry depends on ACE2 and TMPRSS2 and is blocked by a clinically proven protease inhibitor. Cell 181:271–280.e8. https://doi.org/10.1016/j.cell.2020.02.052.

32. Song Y, Liu P, Shi XL, Chu YL, Zhang J, Xia J, Gao XZ, Qu T, Wang MY. 2020. SARS-CoV-2 induced diarrhoea as onset symptom in patient with COVID-19. Gut 69:1143–1144. https://doi.org/10.1136/gutjnl-2020-320891.

33. Lee AC, Zhang AJ, Chan JF, Li C, Fan Z, Liu F, Chen Y, Liang R, Sridhar S, Cai JP, Poon VK, Chan CC, To KK, Yuan S, Zhou J, Chu H, Yuen KY. 2020. Oral SARS-CoV-2 inoculation establishes subclinical respiratory infection with virus shedding in Golden Syrian hamsters. Cell Rep Med 1:100121. https://doi.org/10.1016/j.xcrm.2020.100121.

34. Chandrashekar A, Liu J, Martinot AJ, McMahan K, Mercado NB, Peter L, Tostanoski LH, Yu J, Maliga Z, Nekorchuk M, Busman-Sahay K, Terry M, Wrijil LM, Ducat S, Martinez DR, Atyeo C, Fischinger S, Burke JS, Slein MD, Pessaint L, Van Ry A, Greenhouse J, Taylor T, Blade K, Cook A, Finneyfrock B, Brown R, Teow E, Velasco J, Zahn R, Wegmann F, Abbink P, Bondzie EA, Dagotto G, Gebre MS, He X, Jacob-Dolan C, Kordana N, Li Z, Lifton MA, Mahrokhian SH, Maxfield LF, Nityanandam R, Nkolola JP, Schmidt AG, Miller AD, Baric RS, Alter G, Sorger PK, Estes JD, et al. 2020. SARS-CoV-2 infection protects against rechallenge in rhesus macaques. Science 369:812–817. https://doi.org/10.1126/science.abc4776.

35. Yu J, Li Z, He X, Gebre MS, Bondzie EA, Wan H, Jacob-Dolan C, Martinez DR, Nkolola JP, Baric RS, Barouch DH. 2021. Deletion of the SARS-CoV-2 spike cytoplasmic tail increases infectivity in pseudovirus neutralization assays. J Virol 95. https://doi.org/10.1128/JVI.00044-21.

36. National Research Council. 2011. Guide for the care and use of laboratory animals, 8th ed. National Academies Press, Washington, DC.